

Excited state intramolecular charge transfer reaction in non-aqueous reverse micelles: Effects of solvent confinement and electrolyte concentration[#]

TUHIN PRADHAN, HARUN AL RASID GAZI, BISWAJIT GUCHHAIT and RANJIT BISWAS*

Department of Chemical, Biological and Macromolecular Sciences, and Unit for Nanoscience and Technology, S. N. Bose National Centre for Basic Sciences, JD Block, Sector III, Salt Lake, Kolkata 700 098, India
e-mail: ranjit@bose.res.in

MS received 10 February 2011; revised 31 May 2011; accepted 6 June 2011

Abstract. Steady state and time resolved fluorescence emission spectroscopy have been employed to investigate the effects of solvent confinement and electrolyte concentration on excited state intramolecular charge transfer (ICT) reaction in 4-(1-pyrrolidinyl) benzonitrile (P5C), 4-(1-piperidinyl) benzonitrile (P6C), and 4-(1-morpholenyl) benzonitrile (M6C) in AOT/n-heptane/acetonitrile and AOT/n-heptane/methanol reverse micelles. Dramatic confinement effects have been revealed via a huge reduction (factor ranging between 100 and 20) over bulk values of both equilibrium and reaction rate constants. A strong dependence on the size of the confinement (W_s) of these quantities has also been observed. W_s dependent average static dielectric constant, viscosity and solvation time-scale have been determined. Estimated dielectric constants for confined methanol and acetonitrile show a decrease from the respective bulk values by a factor of 3–5 and viscosities increased by a factor of 2 at the highest W_s considered. Addition of electrolyte at $W_s = 5$ for acetonitrile is found to produce a linear increase of confined solvent viscosity but leads to a non-monotonic electrolyte concentration dependence of average solvation time. Reaction rate constant is found to decrease linearly with electrolyte concentration for P5C and P6C but non-monotonically for M6C, the highest decrease for all the molecules being $\sim 20\%$ over the value in the absence of added electrolyte in the solvent pool. The observed huge reduction in reaction rate constant is attributed to the effects of decreased solution polarity, enhanced viscosity and slowed-down solvent reorganization of the solvent under confinement in these non-aqueous reverse micelles.

Keywords. Intramolecular charge transfer reaction; non-aqueous reverse micelles; confinement effects; static and dynamic solvent control.

1. Introduction

Reverse micelles are formed via self aggregation in a ternary mixture of surfactant, polar and non-polar solvents.^{1–27} A subtle balance between dispersive and electrostatic interactions is the key for the multiple components to remain in a single solution phase. The most commonly used surfactant is sodium *bis* (2-ethylhexyl)-sulfosuccinate (AOT) which possesses charged (anionic) head group and forms both aqueous and non-aqueous reverse micelles in presence of a nonpolar solvent (usually isooctane or heptane). The polar solvents trapped inside reverse micelles behave differently from the pure solvents because geometric

confinement substantially modifies many bulk solvent properties. Eventhough water has traditionally been the most common polar solvent component, a few non-aqueous polar solvents have also been used to form reverse micelles. Use of these non-aqueous polar solvents has been motivated partly by the desire to investigate whether aqueous and non-aqueous reverse micelles behave similarly in solvent encapsulation and partly to employ the confined non-aqueous media as microreactors for certain reactions.^{28–31}

Recently, AOT/isooctane (or heptane)/polar solvent reverse micelles with methanol and acetonitrile as polar liquids have been characterized by dynamic light scattering (DLS) experiments and ultraviolet-visible (UV-vis) absorption spectroscopy.¹⁹ An important issue here is the partial solubility of methanol and acetonitrile in bulk nonpolar solvent (heptane or isooctane)

*For correspondence

[#]The paper is dedicated to the fond memory of Dr. Suhrita Bagchi.

as this allows dispersion of polar solvent into the non-polar phase and thus leading to less swelling of reverse micelle droplets at higher loadings of polar solvents. A correlation between the size of these non-aqueous reverse micelles and ratio (W_s) between concentrations of polar solvent and surfactant ($W_s = [\text{polar solvent}]/[\text{AOT}]$) attempted in this study¹⁹ reveals that while methanol reverse micelles registers an over-all increase in diameter from ~ 3 nm to ~ 5 nm in changing W_s from ~ 1 to 10, the size remains almost unaltered for acetonitrile between W_s values 1 and 5. Absorption data using a dye suggests that, in the above narrow size range, the polar solvents are confined in the cavity formed via the aggregation of surfactant head-groups. However, polar solvent partitioning into the nonpolar phase has been reported at higher values of W_s . Further studies with methanol reverse micelles using Fourier transform infrared (FTIR) spectroscopy^{32,33} indicate the presence of broadly two kinds of methanol molecules-bound and free. While the bound molecules are considered as those found at and within the ionic layer constituted by Na^+ and $-\text{SO}_3^-$ ions, the free ones (bulk type) are residing either at the centre of the cavity or dispersed out into the non-polar phase and existing as monomeric or other aggregated forms. Interestingly, while a few investigators^{19,32} interpret their spectroscopic results in terms of change in size of reverse micelle with W_s , others³³ attribute the observed dependence to the change in shape (for example, spherical to ellipsoid) only. Even though similar studies with acetonitrile reverse micelles have not been carried out yet, dynamic fluorescence Stokes' shift measurements with several coumarin dyes have repeatedly indicated W_s insensitivity for acetonitrile reverse micelles but moderate dependence for above.¹⁹

Addition of electrolyte in confined pool, on the other hand, may affect the environment in many ways. First, phase transition (structural) may occur from oil-in-water (o/w, Winsor I system) type to water-in-oil (w/o, Winsor II system) type via an intermediate phase (Winsor III system).³⁹⁻⁴¹ Therefore, addition of electrolyte in reverse micelles may be used as an experimental control variable where structural transition can be engineered and used for desired product formation.²¹ Second, addition of electrolytes affects the existing electrostatic interactions in a confined pool by supplying additional ions and ion-pairs in the medium.⁴² This leads to the modification in droplet size and its ability to accommodate the host particles. In addition, the viscosity and average polarity of the confined medium are expected to be different in presence of added salts and hence environment response time scale will be

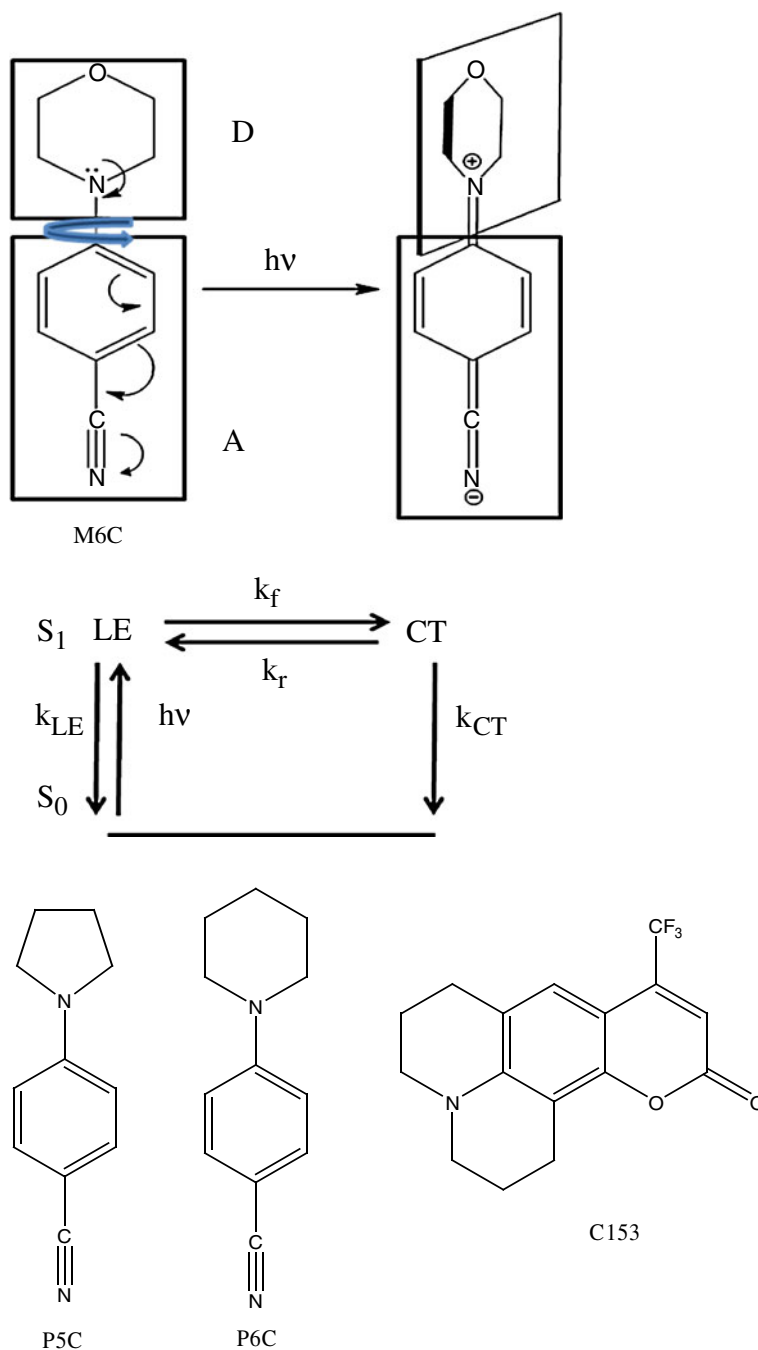
altered. This may impart significant effects on a reaction occurring in such micro-environment in presence of electrolyte.

Recently, photo-induced intramolecular charge transfer (ICT) reaction has been studied in aqueous and several non-aqueous AOT/heptane reverse micelles where the importance of the reverse micelle interface to control an ICT process are stressed.^{22(a),37,43} Another recent study¹⁰ of ICT reaction occurring in aqueous reverse micelles has revealed more than an order of magnitude slowing down of the reaction rate constant in aqueous pool compared to that in a bulk solvent of comparable polarity (in terms of static dielectric constant, ϵ_0) and viscosity. The role of sluggish medium dynamics for lengthening the reaction time constant has been stressed in that work¹⁰ for the first time. However, whether such an effect is also operative for reverse micelles with non-aqueous polar solvents of much lower ϵ_0 , has not yet been studied. Furthermore, effects of electrolyte on an ICT reaction in confined pool needs to be investigated in order to understand the confinement-induced modification of the electrolyte-concentration dependent reaction rate constant of a TICT reaction already measured in bulk electrolyte solutions.⁴⁴⁻⁴⁶ Here, we report such a study where photo-induced intramolecular charge transfer reaction has been investigated in AOT/heptane non-aqueous reverse micelles at different W_s values, and also in presence of electrolytes in confined solvent at a fixed W_s . The non-aqueous polar solvents considered in this study are methanol and acetonitrile which are different in association character but of comparable polarities (ϵ_0 values are 32.66 and 35.94 respectively).⁴⁷ In addition, reverse micelles with these polar solvents are well-characterized.^{19,32,33} Therefore, use of these two solvents will assist in unravelling the role of solvent association character on ICT reaction in confinement.

Three TICT molecules, 4-(1-pyrrolidinyl) benzonitrile (P5C), 4-(1-piperidinyl) benzonitrile (P6C), and 4-(1-morpholenyl) benzonitrile (M6C), are used for the proposed study. The chemical structures of these molecules are shown in scheme 1. Note that earlier study with these molecules in bulk solvents indicate a reaction activation barrier of $\sim 3-4 k_B T$ which is not large enough to inhibit breaking down of conventional kinetics observed in the case of high barrier reaction.^{48,49} Consequently, it would be interesting if one encounters non-exponential reaction kinetics for these molecules in these reverse micelles, as observed earlier for several bulk polar solvents.⁴⁸ Moreover, study with these three TICT molecules is required to establish the generality of the results for a given family of reactant

molecules in these complex environments. As the polarity of a reaction medium plays a very important role in determining both the yield and the rate of ICT reaction in these molecules,⁵⁰⁻⁵⁴ we have made a continuum model estimate of the average polarity (in terms of static dielectric constant, ϵ_0) of the confined polar solvent pool by following the steady state fluorescence emission of a non-reactive polarity probe, coumarin 153

(C153, also shown in scheme 1). Note that extensive spectroscopic investigation with C153 in a wide range of room temperature liquids has revealed that this probe does not participate in specific solute-solvent (such as H-bonding) interaction.⁵⁵⁻⁵⁷ Solution dynamics inside the solvent pool in the reverse micelles has thus been investigated by monitoring the time-evolution of the fluorescence emission of the same probe molecule (C153).



Scheme 1. Pictorial representations of photo-excited intramolecular charge transfer reaction, reaction kinetics and chemical structures of solutes used.

Since solvation time-scale is known to influence reaction rate,^{58,59} estimation of the former is crucial for interpreting the experimental results. We shall shortly see that ICT reaction in these molecules also thought to involve twisting^{48–51} and thus expected to couple to the local ‘stiffness’ of the medium. Fluorescence anisotropy measurements have been carried out to estimate such stiffness or *local* viscosity experienced by the twisting mode while reacting inside a confined pool.

We have used the twisted intramolecular charge transfer (TICT) model^{50,51,60–62} to explain the decay kinetics of these ICT molecules, although alternative arguments can also be employed.^{63–66} Since the mechanism of TICT reaction is already discussed elsewhere,^{48–51} we describe the mechanism very briefly here with the help of scheme 1. Upon photo-excitation, locally excited (LE) state is produced and converted to the relatively more polar charge transfer (CT) state with a forward reaction rate constant, k_f . There may be a barrier involved with the excited state (S_1) conversion from LE state to the CT state.⁴⁸ Subsequently, the CT state can either regenerate the LE state by participating in the reverse reaction with a rate constant, k_r , or, decay to the ground state (S_0) with net (radiative + non-radiative) rate constant, k_{CT} . The photo-prepared LE state is depopulated to the ground state with the net rate constant, k_{LE} . In such a model, LE→CT inter-conversion reaction can be described by a two-state scheme. Additionally, it has been found that the inter-conversion reaction rate is generally faster than the LE and CT decay rates.⁴⁸ In such a situation and in the absence of solvation dynamics on the reaction time scale, it has been shown that the time evolution of the LE or CT population could be described by a bi-exponential function of time.⁴⁸

2. Experimental details

2.1 Sample preparation

P5C, P6C and M6C were synthesized by following literature method.^{61,62} and re-crystallized twice using cyclohexane (Merck, Germany) as solvent. The absence of impurity in these synthesized compounds was ensured via thin layer chromatography (TLC) and monitoring the excitation wavelength dependence of fluorescence emission in several bulk polar and non-polar solvents. Methanol, acetonitrile and LiClO_4 were used as received (highest grade, Aldrich). *Bis*-(2-ethylhexyl) sodium sulfosuccinate (AOT) ($\geq 98\%$, Fluka and Sigma, $\geq 99\%$) was used after vacuum

drying for 24 h. Spectroscopic grade n-heptane (Merck, $\geq 99.5\%$) were used after drying over molecular sieves and filtration. Measured amount of solid AOT was dissolved in n-heptane to make solutions. Subsequently, polar solvent or solution of polar solvent with known electrolyte concentration was added to the solution to obtain appropriate W_s . The concentration of AOT in all reverse micelles was maintained at 0.1 M. The W_s values were restricted up to the limit at which no phase separation was observed and also earlier reports^{19,32–38} of polar solvents being mostly inside the cavity. The highest concentration of added electrolyte (LiClO_4) was restricted at 0.9 M because of instability of reverse micelles at electrolyte concentration larger than 0.9 M.

2.2 Steady state measurements and estimation of spectral properties

Steady state absorption and emission spectra were recorded by using respectively an absorption spectrophotometer (Shimadzu, UV – 2450) and a fluorimeter (SPEX fluoromax – 3, Jobin-Yvon, Horiba). Fluorescence spectra were collected after adjusting the absorbance of the sample to ~ 0.1 (concentration of ICT molecules in solution $< 10^{-5}$ moles-litre⁻¹). Solutions were taken in an optically transparent quartz cuvette with 1 cm optical path length before measurements. For a given sample, the peak wavelength (λ) of the absorption spectrum was used as excitation wavelength for the corresponding emission scan. The fluorescence spectra were corrected for the wavelength dependence of the sensitivity of the apparatus. Solvent background was subtracted from the spectrum of samples. The spectrum was then converted properly to the frequency plane before calculating several steady state properties. Dry argon gas was passed into a few samples and emission spectra were collected. These runs showed very little or no effects on the spectra of charge transfer molecules in solutions and also on the decay kinetics.

LE and CT bands were obtained after deconvolution of the full emission spectrum of the TICT molecules into two fragments by shifting and broadening the reference emission spectrum of the corresponding TICT molecules in a least interacting solvent, which was chosen to be perfluorohexane.⁴⁸ The linewidth of the individual bands (LE and CT) were determined by convoluting the reference emission with a Gaussian line broadening function (inhomogeneous solvent broadening assumed). A given experimental emission spectrum was then least-squared fit to the model spectrum consisting of two bands derived from the shifted and

broadened reference emission spectrum. As seen earlier, this method describes reasonably well both the LE and CT band shapes and allows determination of spectral properties with better accuracy.^{44–46,67–69}

Shifts of the emission spectra from the peak of the reference emission spectra were estimated and added to the *average* peak frequency of the emission spectra to determine the emission peak frequencies of the LE and CT bands. The *average* of the reference emission peak frequency was calculated by averaging the numbers obtained by fitting the upper half of the reference emission spectrum with an inverted parabola, first moment and the arithmetic mean of the frequencies at half intensities on both blue and red ends of the emission spectrum.^{56,70} Absorption peak frequencies were obtained by calculating the first moments of the absorption spectra. The error associated with the peak frequency determination is typically $\pm 250 \text{ cm}^{-1}$ and that with the band area is $\sim 10\%$ (of the reported value), unless otherwise mentioned.

2.3 Reaction time constant measurements

Time correlated single photon counting (TCSPC) technique based on a laser system (Lifespec-ps, Edinburgh, UK) with a light emitting diode (LED) was used to collect fluorescence emission intensity decays. The excitation wavelength was 299 nm and the full width at half maximum (fwhm) of the instrument response function (IRF) ~ 475 ps. Emission decays were collected at both LE and CT peak positions (of steady state spectrum) with an emission band pass of 8 nm at magic angle of 54.7° to avoid effects of solute rotation.⁷¹ Subsequently, the collected emission decays were deconvoluted from the IRF and fitted to bi-exponential functions of time using an iterative reconvolution algorithm.⁵⁵ Such an iterative process is believed to be capable of describing dynamical events approximately 3–5 times faster than the fwhm of the IRF.^{48,72,73} For all W_s values in these non-aqueous reverse micelles and all LiClO_4 concentrations at $W_s = 5$ for acetonitrile, bi-exponential fit to each of the LE emission decays produced one short time constant and one long time constant, whereas each of the CT emission decays (collected wherever possible) fit generated one rise-time (similar to short time constant of LE decay) and one long time constant. Therefore, the short time constant associated with the LE decay was considered as the reaction time. The LE decay of the TICT molecules in non-polar solvents such as in heptane or hexane was found to decay single exponentially with one time constant in the range of a couple of nanosecond. For a few cases, emission decays

were collected at two or three different emission wavelengths around the LE and CT peaks and the analysed data were found to vary within a small uncertainty. All the experiments were performed at room temperature, $295 \pm 0.5 \text{ K}$.

2.4 Dynamic Stokes' shift measurements

About 20 emission decays at equally spaced wavelengths across the steady-state emission spectrum of C153 (solute) dissolved in non-aqueous reverse micelles were collected at magic angle. The collected emission decays were first deconvoluted from the IRF to remove the instrumental broadening and then fitted with a multi-exponential function using an iterative reconvolution algorithm. Time resolved emission spectra (TRES) were then reconstructed from the decay fit parameters.⁵⁵ The time dependent solvation of the laser excited probe was then followed by constructing the normalized spectral or solvation response function⁵⁵

$$S(t) = \frac{\nu(t) - \nu(\infty)}{\nu(0) - \nu(\infty)}, \quad (1)$$

where $\nu(x)$ denotes some measure (first moment or peak) of the time resolved emission spectrum at various time slices. While $\nu(0)$ represents the frequency of the dissolved solute's emission spectrum immediately after excitation, $\nu(\infty)$ denotes the frequency of the emission spectrum after the solvent relaxation is complete (the solute is still in its excited state). Solvation response function, $S(t)$ obtained experimentally was found to be multi-exponential functions of time and the average solvation times were obtained analytically as $\langle \tau_s \rangle = \int_0^\infty dt S(t) = \sum_{i=1}^n a_i \tau_i$.

2.5 Rotation time measurements

Emission decays for time-resolved fluorescence anisotropy ($r(t)$) were collected at the peak wavelength of the steady state emission bands.⁷⁴ Time resolved fluorescence anisotropies, $r(t)$, were calculated from the collected and background subtracted parallel ($I_{\parallel}(t)$) and perpendicular ($I_{\perp}(t)$) decays by using the following well-known formula⁷⁴

$$r(t) = \frac{I_{\parallel}(t) - GI_{\perp}(t)}{I_{\parallel}(t) + 2GI_{\perp}(t)}, \quad (2)$$

where G accounts for the differential sensitivity to the two polarizations which was obtained by tail matching the intensity decays $I_{\parallel}(t)$ and $I_{\perp}(t)$. Note that the

average value for G obtained by tail matching the relevant decays at times longer than the anticipated rotation time is 1.15 ± 0.05 .

The time resolved anisotropy spectra were constructed from the collected emission decays by using Eq. 2 and fitted to functions of the following general form

$$r(t) = r(0) [a_1 \exp(-t/\tau_1) + (1 - a_1) \exp(-t/\tau_2)], \quad (3)$$

where τ_1 and τ_2 in Eq. 3 represent the time constants associated with the decays of the components constituting $r(t)$. Initial anisotropy was denoted by $r(0)$ and was taken as 0.376 for fitting the time resolved anisotropies of C153 in all the concentration in non-aqueous reverse micelles studied here.⁷⁴ Time integration of $r(t)/r(0)$ then produces the average rotation time: $\langle\tau_r\rangle = a_1\tau_1 + (1 - a_1)\tau_2$.

3. Results

3.1 Characterization of the reaction medium

3.1a *Estimation of the average ϵ_0 of the confined pool:* As solution polarity strongly influences an ICT reaction mainly via modifying the reaction barrier,⁴⁸ we have estimated the average dielectric constant (ϵ_0) of the polar solvent confined in AOT/n-heptane/acetonitrile and AOT/n-heptane/methanol reverse micelles by using the following empirical relation^{10,56}

$$\nu_{em} (10^3 \text{ cm}^{-1}) = \nu_g^{em} - A [(\epsilon_0 - 1) / (\epsilon_0 + 2)] - B [(n^2 - 1) / (n^2 + 2)], \quad (4)$$

where ν_{em} represents the emission peak frequency of C153 dissolved in confined solvent pool, ϵ_0 the average static dielectric constant, n the refractive index of the solvent. Fit^{10,56} to liquid data for C153 produces $\nu_g^{em} = 23.12$, $A = 5.06$ and $B = 1.5$. The value of ϵ_0 estimated by using Eq. 4 for non-aqueous solvent pools are shown as a function of W_s in the upper panel of figure 1. It is evident from this panel that the estimated dielectric constants of confined acetonitrile and methanol at the largest W_s are reduced by factors of ~ 5 and ~ 3 , respectively. The reduction at smaller W_s is even more drastic where the estimated dielectric constant is approximately an order of magnitude less than that at the bulk. Such a drastic reduction of bulk dielectric constant upon confinement has also been reported earlier for water^{10,75} and model solvents.^{76,77} This confinement-induced reduction of ϵ_0 can be under-

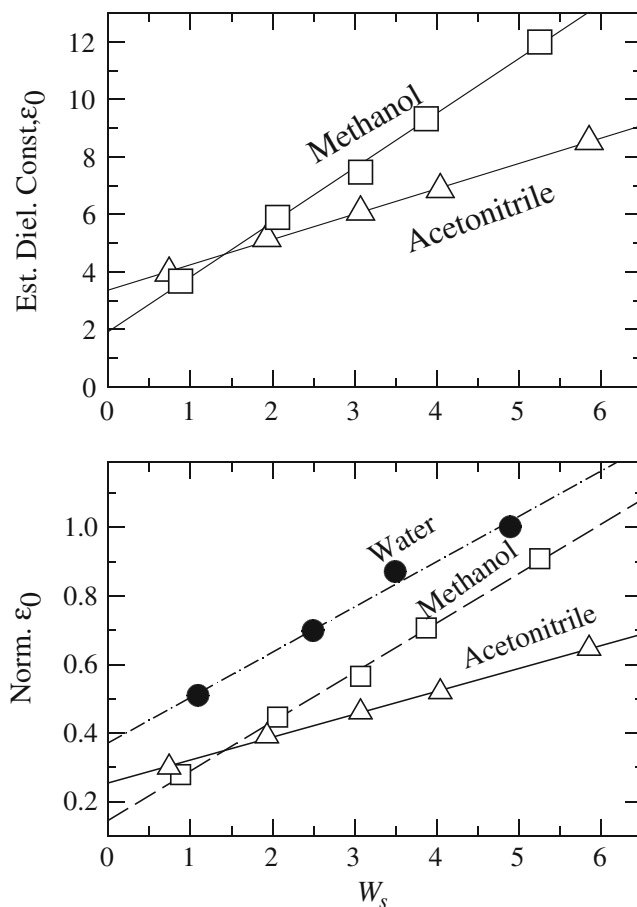


Figure 1. W_s dependence of static dielectric constant (ϵ_0) for confined solvents in AOT/n-heptane/acetonitrile and AOT/n-heptane/methanol reverse micelles in upper panel. Values of ϵ_0 at different W_s values are obtained by using the fluorescence spectral shift of a non-reactive solvation probe, coumarin 153 (C153) in Eq. 4 of the text. The lines going through the symbols (triangles and circles) are obtained from non-linear regression fits and can be described by the following parameters: for methanol, intercept = 1.92, slope = 1.90 and correlation coefficient (R) = 0.99; for acetonitrile, intercept = 3.17, slope = 0.93 and correlation coefficient (R) = 0.99. Comparison of the growth of ϵ_0 with W_s among confined water, acetonitrile and methanol (lower panel). For each solvent, the estimated ϵ_0 has been normalized by the respective value at the highest pool-size shown here.

stood by recalling that the magnitude of the mean-squared fluctuations in the collective dipole moment ($\langle\delta M^2\rangle = [M^2] - \langle M \rangle^2$) determines ϵ_0 through the relation,^{78,79} $[\epsilon_0 - 1] \propto V^{-1} \langle\delta M^2\rangle$, where the collective dipole moment of the system (\mathbf{M}) of volume V is connected to the individual molecular dipole moment (μ_i) as follows, $\mathbf{M} = \sum_i \mu_i$. Since $\langle\delta M^2\rangle \sim N$ (N being the number of polar solvent molecules), it is only natural that the dielectric constant would be significantly reduced (compared to the bulk values) at smaller

W_s where lesser number of polar solvent molecules are present. This relation further suggests a *linear* increase of ϵ_0 of the confined solvent with W_s . This is indeed the case for methanol, acetonitrile and water as reflected in the data shown in the lower panel of figure 1. This linearity breaks down at higher values of W_s for confined water¹⁰ probably because of solute's increasing expulsion from the core to the cavity interface due to interaction of the dipolar solute with ionic surface and increased hydrophobic interaction.

The observed linear dependence for confined acetonitrile on W_s is interesting as earlier studies¹⁹ indicate confined solvent pool does not grow with W_s when acetonitrile is used to form reverse micelles. However, several spectroscopic measurements^{19,34–38} using different coumarin dyes in these non-aqueous reverse micelles have reported red-shift in absorption and fluorescence spectra with W_s , shifts being relatively smaller for acetonitrile than those measured for methanol reverse micelles. Similar results have also been observed in the present study which are reflected in the linear increase of estimated ϵ_0 with W_s and uniformly lower values of it (estimated ϵ_0) for confined acetonitrile than methanol between $1 < W_s < 6$. Moreover, absorption and fluorescence emission spectra recorded at W_s values in this range for acetonitrile reverse micelles (figure S1, Supporting Information) do not indicate any solute partitioning between polar and non-polar phases. For methanol reverse micelles also, spectral shapes do not indicate such partitioning (spectra not shown here). These observations are similar to earlier reports^{19,34–38} and, therefore, suggests that dipolar interactions among polar solvent molecules, solute–solvent dipolar interaction and interactions of the ionic surface with the dipolar solute and dipolar solvent molecules lead these species (dipolar solute and solvent) to reside largely inside the cavity.

The lower panel of figure 1 also indicates that the slopes of variation of dielectric constant with W_s are similar for methanol and water but very different from that for acetonitrile. This may be linked to the partial restoration of hydrogen bonding (H-bonding) network in methanol at larger W_s , which is completely absent for the polar aprotic solvent, acetonitrile. The similar slopes for water and methanol further supports the notion that increase in W_s induces progressive partial restoration of the confinement-disrupted H-bonding network, which, in turn, introduces steeper slopes for the increase of ϵ_0 in these network solvents. The confinement-induced disruption of H-bonding network has been observed in many earlier studies and suggested to be responsible for depression of freezing

transition temperature of water.^{80–84} It is to be mentioned here that the estimated dielectric constant reported here may not represent the ‘true’ value because ions present in the pool can also induce fluorescence shift, which, in the present calculation scheme, is considered as that by dipolar solvents. In addition, spectral shift depends on probe-location in such heterogeneous media and thus the estimated value may vary slightly if one changes the excitation wavelength.^{85,86}

3.1b Solvation time scale of confined polar solvent pool: Average solvation times at several W_s values for acetonitrile and methanol reverse micelles have already been measured via dynamic Stokes' shift experiments.^{34–38} Stokes' shift dynamics in confined methanol and acetonitrile have been found to be at least three orders of magnitude slower than that of the bulk. In addition, these studies report that dynamics become faster for methanol with W_s but remains insensitive for acetonitrile. Our measurements using C153 as probe in AOT/n-heptane/acetonitrile reverse micelles at $W_s = 5$ produce a dynamic Stokes' shift of $\sim 800 \text{ cm}^{-1}$ which is in semi-quantitative agreement with the data reported earlier.³⁴ The measured average solvation time ($\langle \tau_s \rangle$) at this pool size has been found to be ~ 2000 times slower compared to that for bulk acetonitrile with the same probe molecule.⁵⁵ This is also in qualitative agreement with general results from dynamic Stokes' shift measurements for polar solvents under confinement.^{2–7,34–38}

Although we have not repeated the measurements of W_s dependent Stokes' shift dynamics for confined methanol and acetonitrile, we have measured the electrolyte concentration dependence of it in confined acetonitrile at $W_s = 5$. The results are presented in figure 2 where the average solvation time ($\langle \tau_s \rangle$) shows a non-monotonic electrolyte (LiClO_4) concentration dependence. Note that the time scale obtained in our time-resolved measurements is significantly faster than what has been observed in similar pool size ($W_s = 4$) in the absence of added electrolyte.³⁴ This is somewhat perplexing as addition of electrolyte is expected to slow down the rate of solvation.⁷³ One reason could be that the present analyses consider spectral evolution only up to the time when $\nu(t)$ matches that from steady state fluorescence experiments (ν_{em}). The consideration of $\nu(t = \infty) \equiv \nu_{em}$ leaves out a dynamic Stokes' shift of $\sim 200 \text{ cm}^{-1}$ from the total spectral relaxation. Moreover, this part has been found to relax with a time constant of a few to several nanoseconds. While this extremely slow relaxation occurring with a time

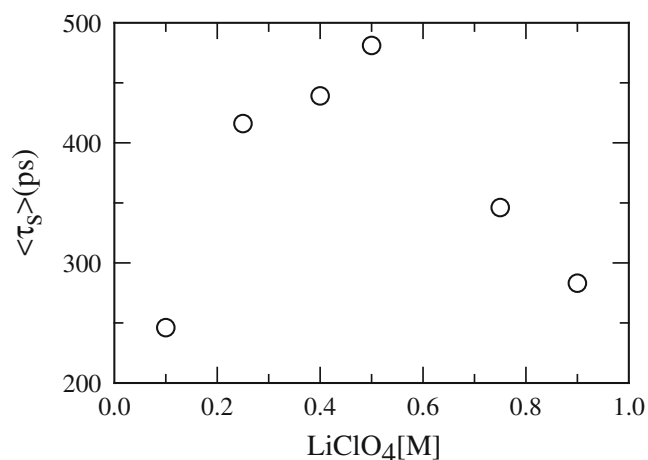


Figure 2. Electrolyte (LiClO₄) concentration dependence of average solvation time in AOT/n-heptane/acetonitrile reverse micelles at $W_s = 5$. C153 has been used as a solvation probe.

constant of few to several nanoseconds may be real for these heterogeneous media, this small amount of dynamic shift ($\sim 200 \text{ cm}^{-1}$) can also arise from a modification in the vibronic structure of the line-shape due to difference in interaction with the environment of the probe in its ground and excited states.⁵⁵

The increase in $\langle \tau_s \rangle$ at low LiClO₄ concentration in figure 2 is because of enhancement of medium viscosity and increased participation of the diffusive ion-solvent exchange dynamics⁷³ in the near vicinity of the dipolar probe. After a certain concentration, further addition of electrolyte may produce more number of ion-pairs which can significantly enhance the average polarity of the confined pool. Such a scenario has already been observed while studying Stokes shift dynamics in bulk ethyl acetate ($\epsilon_0 \sim 6$) in presence of LiClO₄ at various concentrations.⁴² Therefore, the decrease in $\langle \tau_s \rangle$ at higher electrolyte concentrations may be attributed to the increased average medium polarity and additional participation of rotational modes (via the rotation of ion-pairs).⁸⁷ Note the decrease in $\langle \tau_s \rangle$ upon further addition of electrolyte at higher concentrations has also been observed in experiments with electrolyte solutions of strongly polar solvents.⁷³ Application of Fee–Maroncelli method⁸⁸ further suggests that the present experiments have missed, on an average, $\sim 40\%$ of the total shift (table S1, Supporting Information) at this pool size for all these LiClO₄ concentrations. It is to be mentioned here that dynamic light scattering (DLS) measurements indicate a fluctuation in the pool size with LiClO₄ concentration but the size fluctuation always remains within $\pm 20\%$ of the pool diameter in the absence of electrolyte.

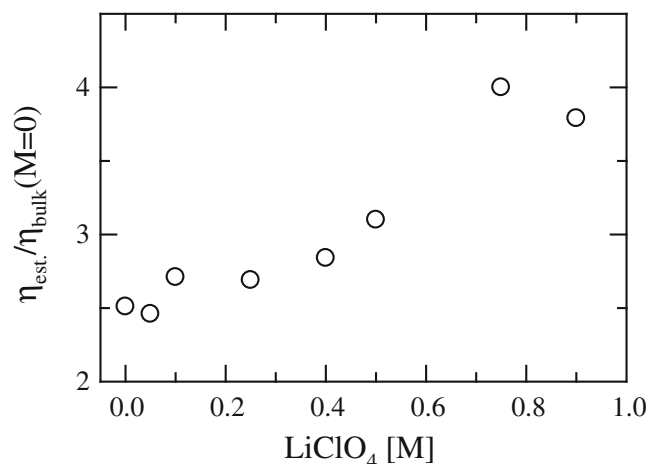


Figure 3. Electrolyte-induced enhancement of pool viscosity in AOT/n-heptane/acetonitrile reverse micelles at $W_s = 5$. Ratio between the estimated viscosity ($\eta_{est.}$) of confined acetonitrile at this W_s and that ($\eta_{bulk}[M = 0]$) of bulk pure acetonitrile are shown as a function of electrolyte (LiClO₄) concentration. Values of $\eta_{est.}$ have been determined from the measured rotation times of C153 dissolved in the reverse micelle droplets.

3.1c Estimation of local viscosity: Local viscosity experienced by the probe in reverse micelles droplets has been estimated by using the correlation, $\langle \tau_r \rangle = (58.1 \pm 1.6) \eta^{0.96 \pm 0.03}$, constructed from the rotation data of the same probe in bulk polar protic and aprotic solvents at room temperature.⁷⁴ Note in the above correlation, average rotational time $\langle \tau_r \rangle$ is in picosecond

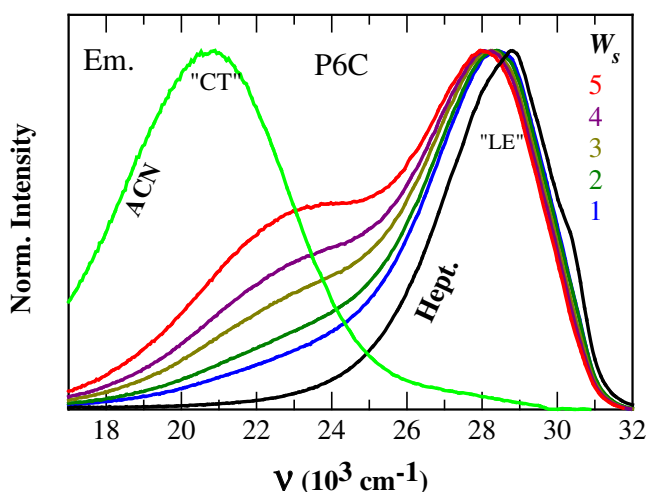


Figure 4. W_s dependence of fluorescence emission spectrum of one of the ICT molecules, P6C dissolved in acetonitrile reverse micelles. The spectra are colour-coded. Emission spectra of the same molecule in acetonitrile and heptane are also shown. 'LE' represents the locally excited state and 'CT' the charge-transferred state.

(ps) and η is in centipoise (cP).⁸⁹ Our measured $\langle\tau_r\rangle$ for C153 in AOT/heptane/acetonitrile reverse micelles at $W_s = 5$ in the absence of any added electrolyte compares well with the existing data (~ 60 ps versus ~ 80 ps at $W_s = 4$ ³⁵). Corresponding bi-exponential fit parameters for the measured $r(t)$ are summarized in table S2 (Supporting Information). Electrolyte concentration dependent viscosity of the confined acetonitrile at $W_s = 5$ is then extracted by inserting the measured $\langle\tau_r\rangle$ into the above correlation. The results are presented in figure 3 where a near linear increase of estimated viscosity with LiClO_4 concentration is indicated. Note the estimated viscosity ($\eta_{est.}$) at $W_s = 5$ in the absence of electrolyte is nearly twice as large as that of bulk pure acetonitrile (η_{bulk} [$M = 0$] = 0.34 cP) which, upon further addition of electrolyte, enhances by a factor of 4. However, such an interpretation of slowed-down rotation time of a polar probe in terms of enhanced viscosity assumes negligible or no frictional resistance arising from the longer-ranged solute–solvent dipolar interaction and solute-ion dipole-ion

interaction.⁹⁰ A number of experimental^{74,91} and simulation studies^{92–94} in highly polar conventional solvents have shown that longer-ranged interactions play a minor role in rotational friction. Mechanical friction from short-ranged interactions, its enhancement via electrostatic interactions (or electrostriction), and in some cases, specific solute–solvent interactions, principally govern the rotational time scale.

3.2 ICT reaction in confined polar solvent

3.2a *Reaction equilibrium constant and free energy (W_s dependence):* Representative emission spectra of P6C in AOT/n-heptane/acetonitrile reverse micelles at different W_s values are shown in figure 4. For comparison, emission spectra of the same ICT molecule in acetonitrile and heptane are also shown in the same figure. It is evident from this figure that as W_s increases, the emission spectrum red-shifts with simultaneous growth in the charge-transferred (CT) band. The CT band

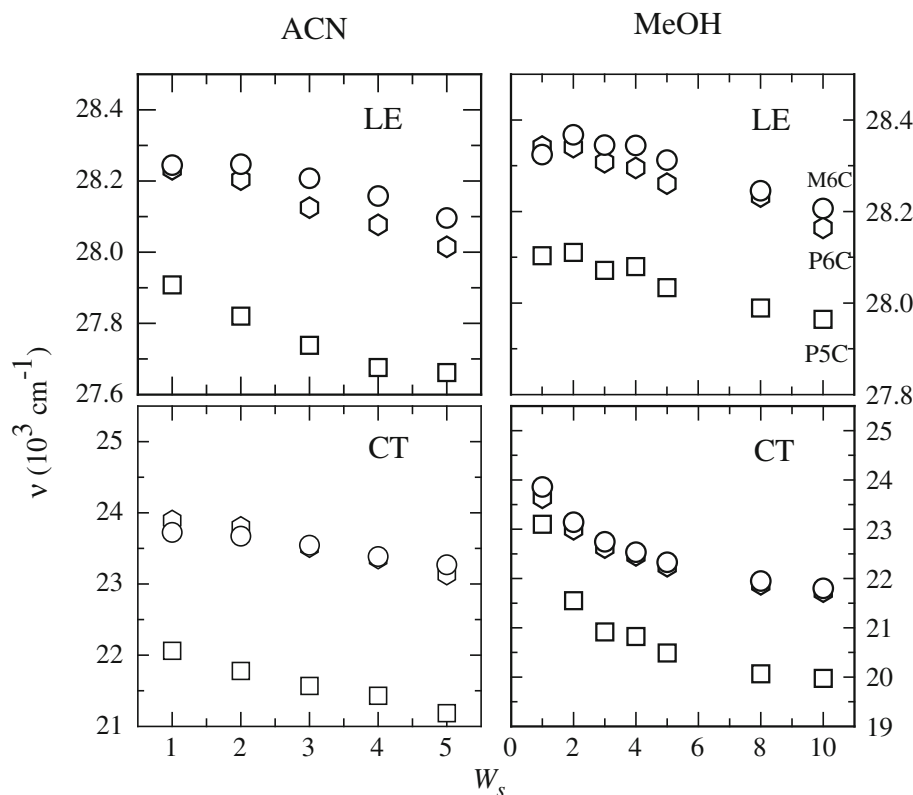


Figure 5. W_s dependence of the LE and CT emission peak frequencies of P5C, P6C and M6C in AOT/n-heptane/acetonitrile and AOT/n-heptane/methanol. Non-aqueous solvents acetonitrile (left panel, ‘ACN’) and methanol (right panel, ‘MeOH’) are indicated. Symbols (circles, hexagons and squares) tagged with solute identity in the upper-right panel describe the data for P5C, P6C and M6C in all the four panels. The estimated uncertainty in frequency is ± 300 cm^{-1} .

becomes most prominent at the highest W_s considered. Since it is known that medium polarity facilitates the formation of CT state,¹⁰ the continuous growth in CT population with W_s may be attributed to the continuous enhancement of medium polarity at higher loading of polar solvent. The role of medium polarity in forming the CT population is further supported by the observation that photo-excitation of M6C predominantly produces either CT population in bulk acetonitrile ($\epsilon_0 \sim 36$) or LE in bulk heptane ($\epsilon_0 \sim 2$). Spectral shift and CT band formation, therefore, indicate that the ICT molecule (P6C in this case) is indeed trapped in the solvent pool and interacting with the immediate environment. However, solute partitioning into the non-polar and micellar pseudophases^{9,29} could be an issue here as this will lead to emission at different energies producing an emission profile similar to the ones displayed in figure 4. However, the peak-to-peak difference between

the emission spectra of P6C in acetonitrile and heptane is much larger ($\sim 8000 \text{ cm}^{-1}$) than that in the largest pool ($\sim 5000 \text{ cm}^{-1}$, see also figure 5). In addition, the peak frequency of the CT emission band at any of the W_s considered is blue-shifted at least by $\sim 3000 \text{ cm}^{-1}$ than that in bulk acetonitrile. Moreover, the absorption spectra of this molecule at various W_s , shown in figure S2 (Supporting Information) do not indicate any distribution of the polar solvent out into the non-polar phase. All these observations suggest that the emission spectra of P6C in these reverse micelles are predominantly originating from those dissolved inside the confined polar solvent pool.

The W_s dependences of the LE and CT emission peak frequency of the three TICT molecules in AOT/n-heptane/acetonitrile and AOT/n-heptane/methanol reverse micelles are shown in figure 5. In both these non-aqueous reverse micelles, the LE and CT peak

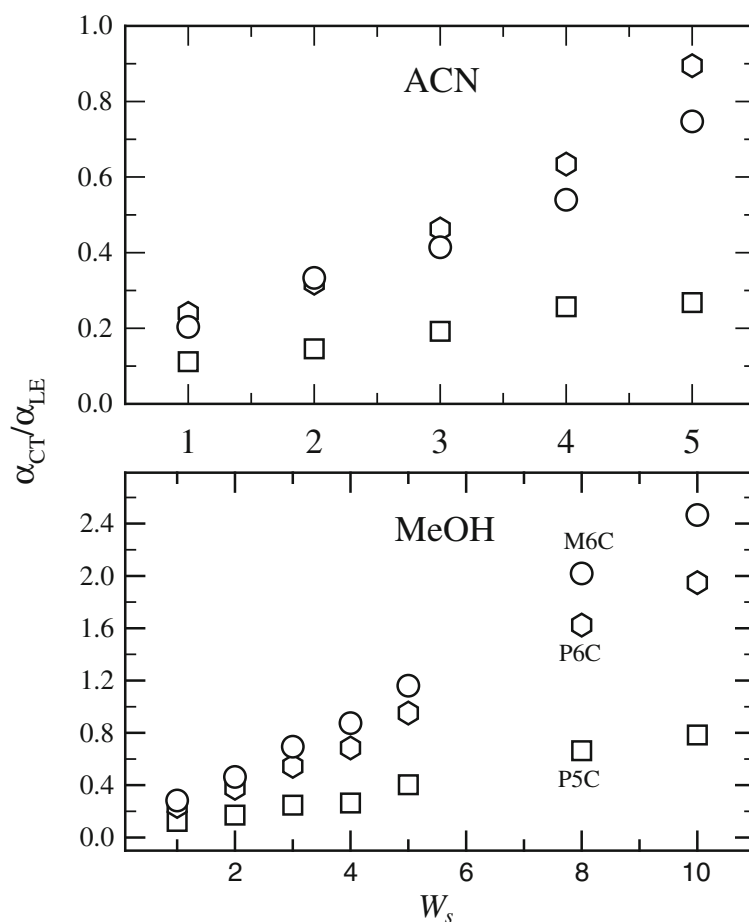


Figure 6. W_s dependence of the ratio between the areas under the CT and LE emission bands (α_{CT}/α_{LE}) of P5C, P6C and M6C in AOT/n-heptane/acetonitrile and AOT/n-heptane/methanol. Identity of the non-aqueous polar solvents used is indicated in each panel. The uncertainty for CT band area is typically within $\pm 10\%$.

frequencies show red-shift with increase in pool size (see also table S3, Supporting Information). The total shift for the LE emission peak is much less and it is about $\sim 200\text{ cm}^{-1}$ for all these ICT molecules in these two types of reverse micelles. The total CT shift, on the other hand, is much larger and is $\sim 1000\text{ cm}^{-1}$ for both acetonitrile and methanol at $W_s = 5$. In both these non-aqueous reverse micelles the regularity in spectral shifts (particularly for the CT band) with W_s again suggests continuous increase of polarity around the trapped solute. The CT shift becomes even larger ($\sim 2000\text{--}3000\text{ cm}^{-1}$) for methanol because one can reach $W_s = 10$ with this solvent. Interestingly, the total CT shift in methanol reverse micelles is very similar to earlier

observations for M6C in aqueous reverse micelles.¹⁰ However, the LE peak frequency of closely related ICT molecules in neat solvents⁴⁸ exhibited blue-shift with concomitant narrowing of the emission band, whereas in these non-aqueous reverse micelles the LE band redshifts with simultaneous broadening (see table S3). While the heterogeneity in the environment around the confined reactant in these reverse micelles can contribute to the spectral broadening, the observed redshift in LE band may arise due to the spectral broadening rather than from any fundamental difference in solute-environment interaction between neat and confined solvents. However, the uniform nature of the LE peak frequency versus LE-width correlation observed in the

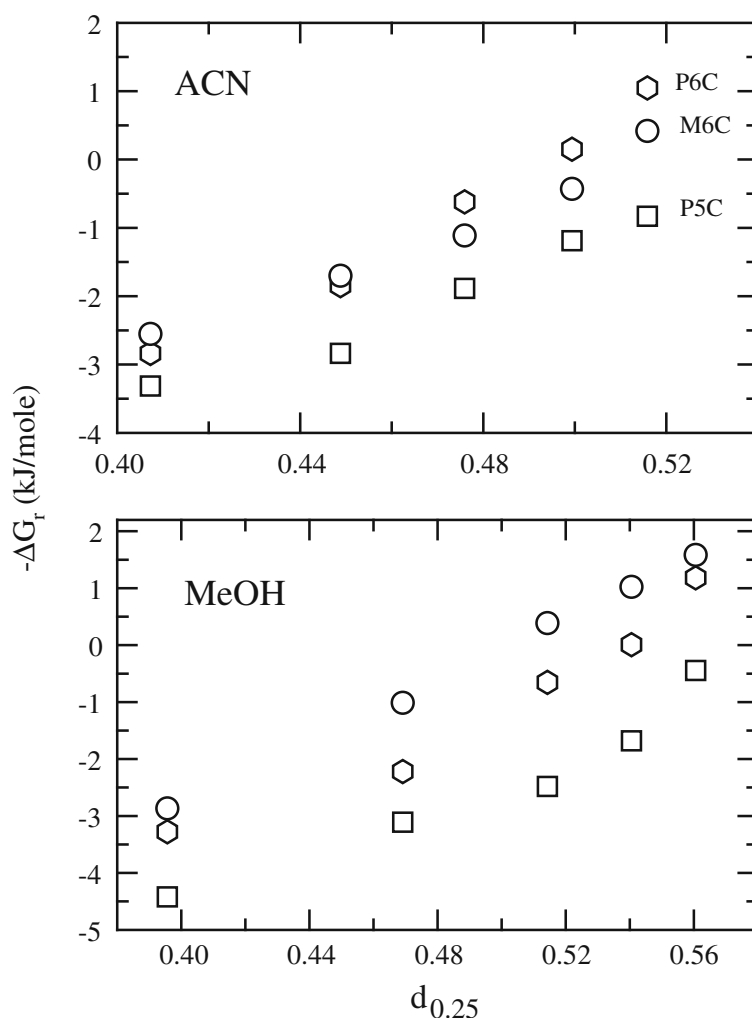


Figure 7. The correlation between the reaction driving force ($-\Delta G_r$) and a dielectric field factor, $d_{0.25}$ for the LE \rightarrow CT conversion reaction of P5C, P6C and M6C molecules in AOT/n-heptane/acetone nitrile (*upper panel*, 'ACN') and AOT/n-heptane/methanol (*lower panel*, 'MeOH') reverse micelles. Values of the dielectric constant for the confined solvent used are those shown in figure 1. The symbols (hexagon, circle and square) are solute-tagged.

present study warrants further investigation. The correlation between CT peak shift and bandwidth for these molecules in these reverse micelles is similar as that observed not only in aqueous reverse micelles¹⁰ but in bulk polar solvents^{48,68,69} and electrolyte solutions^{45,46,67} also.

Since the photo-induced LE→CT reaction in these molecules is favoured by the polarity of a reaction medium,⁴⁸ the ratio between the areas under these two bands (α_{CT}/α_{LE}) is expected to increase with W_s . Figure 6 reflects indeed such results where α_{CT}/α_{LE} for P5C, P6C and M6C in these non-aqueous reverse micelles are shown as a function of W_s . The area ratios for these ICT molecules have been drastically reduced under confinement compared to those in the respective bulk polar solvents. For example, α_{CT}/α_{LE} for P6C in the smallest and largest W_s values for acetonitrile correspond to those found in bulk diethyl ether ($\epsilon_0 \sim 4$) and bulk decanol ($\epsilon_0 \sim 7$)⁴⁸ but ~ 100 to ~ 10 times less than that in bulk acetonitrile. Moreover, in the acetonitrile-saturated solution of heptane α_{CT}/α_{LE} for P6C is found to be ~ 4 times less than that at $W_s = 5$. Data shown in the lower panel of figure 6 indicate substantial reduction in α_{CT}/α_{LE} for these ICT molecules in confined methanol also. The reduction in α_{CT}/α_{LE} values in these confined solvents therefore follow the trend of change in ϵ_0 upon confining these polar solvents but the extent of decrease is much larger than the corresponding decrease in ϵ_0 . This indicates that the solvent control of an ICT reaction in confined solvents is more complicated than that when the reaction occurs in bulk media.

Next, a correlation between the change in free energy for the photo-induced LE→CT conversion reaction ($-\Delta G_r$) in these ICT molecules and a dielectric reaction field factor (d_c) is explored in figure 7 for these non-aqueous reverse micelles. The following representative field factor, $d_c(\epsilon_0) = \frac{\epsilon_0 - 1}{2(1-c)\epsilon_0 + (1+2c)}$, is employed for such a correlation where the W_s dependent ϵ_0 is used. The parameter c , ranging between 0 and 1, effectively accounts for solute polarizability effects.⁴⁸ A value of 0.25 for c has been used here since this has been found to produce the best correlation for reactions in bulk solvents.⁴⁸ The driving force ($-\Delta G_r$) for the reaction is obtained from the reaction equilibrium constant (K_{eq}) by using the relation, where K_{eq} has been calculated from the arithmetic mean of the equilibrium constant determined from the steady state data⁴⁸ ($K_{eq}^\phi \approx \frac{\alpha_{CT} v_{LE}^3}{\alpha_{LE} v_{CT}^3}$) and time-resolved experiments ($K_{eq}^a = a_{rxn}/a_{dec}$). Note that a_{rxn} and a_{dec} are respectively the amplitudes associated with the short

(reaction) time and the long time components of the time-resolved emission (population) decay. Note that the W_s dependent $-\Delta G_r$ varies from negative to positive indicating that a less favourable LE→CT conversion reaction in smaller W_s becomes more favourable in larger W_s . In addition, a near linear correlation between $-\Delta G_r$ and d_c suggests that the trapped reactants are experiencing more polar environment upon increasing W_s , and medium polarity influences an ICT reaction in confined solvents in qualitatively the same way as in bulk media.

3.2b Effects of salt concentration on reaction at a fixed W_s : Effects of electrolyte on LE→CT conversion reaction occurring in confined polar solvent pool is studied next. Figure 8 depicts the LiClO₄ concentration dependences of area ratio (α_{CT}/α_{LE}) and reaction driving force ($-\Delta G_r$) for the conversion reaction in all these molecules in AOT/heptane/acetonitrile reverse

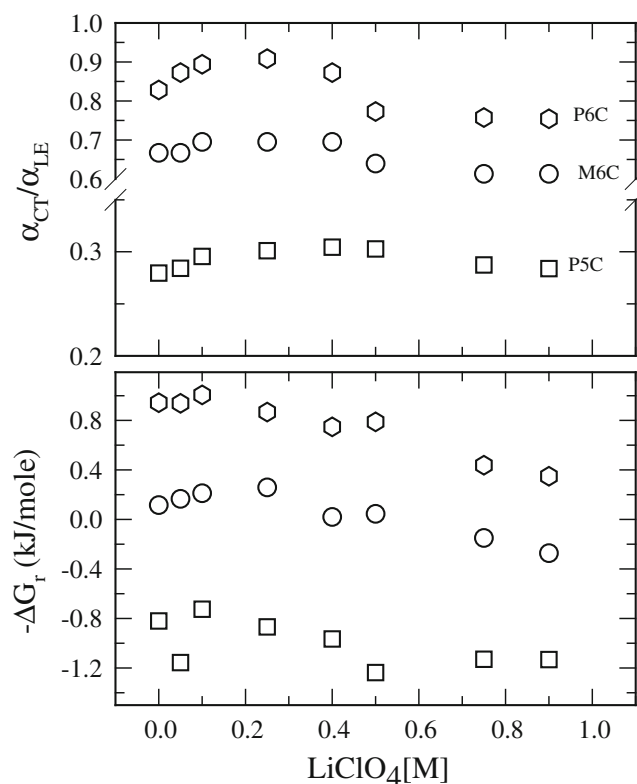


Figure 8. Electrolyte (LiClO₄) concentration dependence of area ratio, α_{CT}/α_{LE} and reaction driving force ($-\Delta G_r$) in these ICT molecules in AOT/heptane/acetonitrile reverse micelles at $W_s = 5$. $-\Delta G_r$ is obtained from the average equilibrium constants which is an arithmetic mean of the equilibrium constants determined from the steady state and time resolved experiments. As before, symbols are solute-tagged.

micelles at $W_s = 5$. Electrolyte effects on peak frequencies and widths are found to be very small (see figure S3, Supporting Information). However, it is evident from the upper panel of figure 8 that the area ratio varies non-monotonically with electrolyte concentration, degree of non-monotonicity being the strongest for P6C and weakest for P5C. A small variation in activation energies⁴⁸ of these molecules and the subsequent difference in medium control might be responsible for such a behaviour. The skewedness is somewhat softened in the lower panel because of logarithmic relationship between $-\Delta G_r$ and α_{CT}/α_{LE} . Interestingly, such a non-monotonic dependence of average solvation time on electrolyte concentration at this pool size has already been observed (figure 2) and it is quite likely that these two are connected. We shall explore more on this issue when we describe results from time-resolved studies.

3.2c Reaction rate constant: W_s dependence: The W_s dependence of the LE \rightarrow CT reaction rate constant of P5C, P6C and M6C has been studied in both AOT/heptane/acetonitrile and AOT/heptane/methanol reverse micelles. Time-resolved fluorescence intensity decays for M6C in methanol reverse micelles at a few W_s values are shown in figure 9. The decay pattern reflects a considerable W_s dependence. Similar W_s

dependence of intensity decay has also been observed for reaction occurring in confined acetonitrile (decays not shown here). As already discussed, the reaction rate constants have been determined by fitting the collected LE and CT emission intensity decays to bi-exponential functions of time. A pair of such representative fits are displayed in figure 10 for M6C in methanol reverse micelles at $W_s = 5$. The fitted data along with the instrument response function and the residuals are also shown in the same figure. Similar values for the fast time constant (τ_1) associated with the LE-decay and CT-rise suggest that τ_1 indeed represents the reaction time constant ($\tau_{rxn} = 1/k_{rxn}$, k_{rxn} being the reaction rate constant) associated with the LE \rightarrow CT conversion reaction. In addition, adequacy of just two exponentials in describing the decay kinetics also suggests that the reaction proceeds via the same mechanism in these reverse micelles as observed in bulk acetonitrile and methanol.^{48,49} Most interestingly, the reaction time constant of ~ 450 ps at this W_s is ~ 30 times longer than that measured with the same molecule (M6C) in bulk methanol (~ 15 ps).⁴⁹ In saturated methanol or acetonitrile solutions of heptane, τ_{rxn} for M6C has been found to be ~ 10 times longer than in bulk pure polar solvents. This lengthening of τ_{rxn} in saturated binary mixtures is mainly due to the reduction in solution polarity.⁵²⁻⁵⁴ The fact that τ_{rxn} at $W_s = 5$ is ~ 3 times larger than that in binary mixtures (~ 450 ps versus

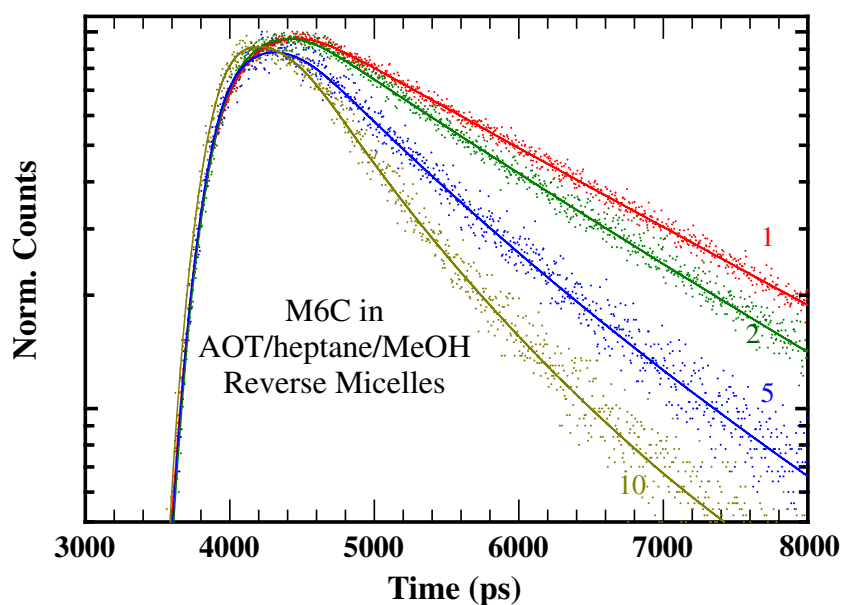


Figure 9. Pool-size dependence of time-resolved population decay of M6C in AOT/heptane/methanol reverse micelles. The figure is colour-coded. Number attached to each decay denotes a value of W_s at which intensity decay has been collected.

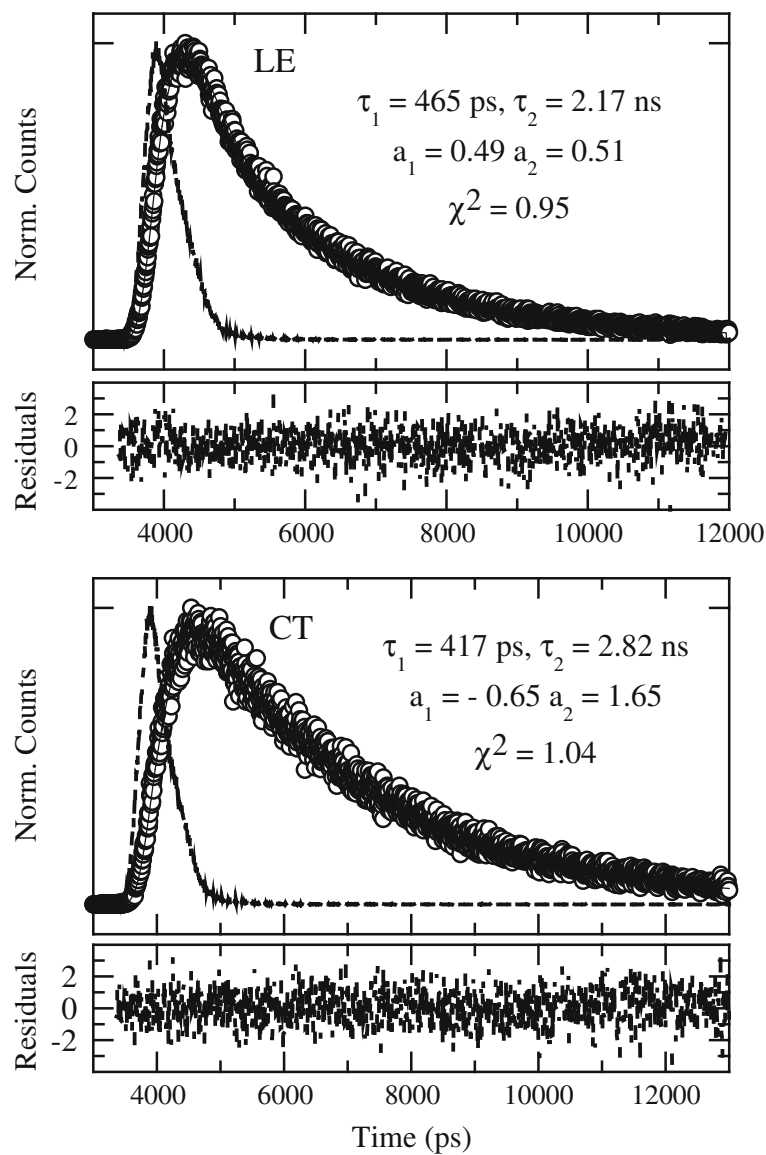


Figure 10. Representative LE emission decay (*upper panel*) and CT emission decay (*lower panel*) of M6C in AOT/n-heptane/methanol reverse micelles at $W_s = 5$ and their bi-exponential fits. While the experimental data are represented by circles, fits through the data points are shown by solid lines. The instrument response function is shown by the broken line. χ^2 denotes the ‘goodness-of-fit’ parameter. The LE peak count is ~ 3000 and CT peak count is ~ 1000 . Residuals are shown in the bottom of each panel.

~ 150 ps) clearly indicates the measured reaction time is indeed associated with the reaction occurring in confined polar solvents.

While the W_s dependent reaction time constants (τ_{rxn}) are given in Supporting Information (figure S4), the ratio between the reaction time constants in confined and bulk solvents, $\tau_{rxn}(RM)/\tau_{rxn}(bulk)$, obtained for various W_s values are shown in figure 11. Data shown in this figure indicate substantial lengthening of τ_{rxn}

in these non-aqueous reverse micelles for all the ICT molecules considered here and the extent of lengthening, depending on solute and W_s , ranges between ~ 100 and ~ 10 . In addition, τ_{rxn} becomes faster by nearly a factor of 2 in these reverse micelles for changing W_s from 1 to 5. Similar changes in ‘local viscosity’ are also reflected in the pool-size dependent rotation times measured with polar probes in these non-aqueous reverse micelles.^{34,38,95} For methanol, this enhancement

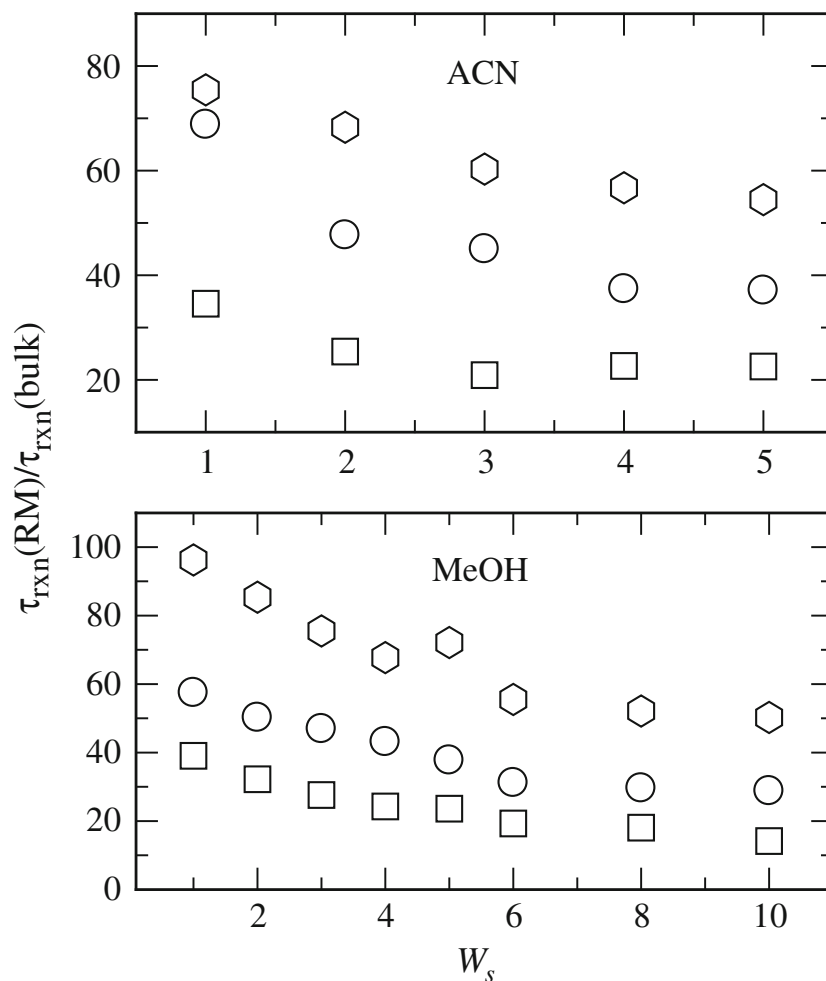


Figure 11. W_s dependence of ratio between reaction time constant, $\tau_{rxn}(RM)/\tau_{rxn}(bulk)$, associated with the LE→CT conversion reaction of P5C, P6C and M6C in AOT/n-heptane/acetonitrile (upper panel) and AOT/n-heptane/methanol reverse micelles (lower panel), and reaction time in bulk acetonitrile and methanol. Note that the squares, hexagons, circles represent data respectively for P5C, P6C and M6C. Error associated with the reaction time constants is typically $\pm 5\%$ of the reported values.

factor doubles to ~ 4 as one can go up to $W_s = 10$ with this alcohol solvent. Interestingly, earlier measurements³⁷ of the non-radiative rate constant for C152 in methanol and acetonitrile reverse micelles showed much less reduction and very weak dependence on W_s . Therefore, the observed huge lengthening of τ_{rxn} upon confinement and substantial variation of it (τ_{rxn}) with W_s are new results and completely different from earlier reports.³⁷ The presence of a sizeable activation barrier and tuning of it with solution polarity, and coupling of the twisting (reactive) mode to local viscosity have probably made the LE→CT conversion reaction of these ICT molecules more sensitive to both the confinement and size of it.

Although τ_{rxn} exhibits acceleration by a factor 2 to 4 upon increasing W_s and follows the associated viscosity changes, the huge reduction of it over the bulk values suggests a much stronger dynamical solvent control of the LE→CT reaction in these ICT molecules. This can be understood qualitatively from the following example. At $W_s = 5$, the solvent polarity (sensed by the solute) is reduced by a factor of ~ 5 and the viscosity enhanced by a factor of ~ 2 . Had these two factors been the only reasons to influence the ICT reaction in M6C and acted in multiplicative manner, then the slowing down of τ_{rxn} (over the bulk value) at $W_s = 5$ would have been merely a factor of ~ 10 . The extent of reduction being much larger (ranging between 100 and

20) than this only supports the conjecture that severely slowed down solvation response (by a factor of 1000 or even more) in these confined systems does not allow the reaction to occur in a fully solvent-relaxed state. This, in turn, indicates a critical role for slow solvation response in determining the rate of ICT reaction occurring in confined media. Further study is thus required to

quantify and separate out the effects of slow solvation on such reactions occurring in reverse micelles.

3.2d *Reaction at a fixed W_s : Electrolyte effects:* Figure 12 shows the electrolyte (LiClO_4) concentration dependence of reaction time constant (τ_{rxn}) for P5C, P6C and M6C in AOT/n-heptane/acetonitrile reverse micelles at

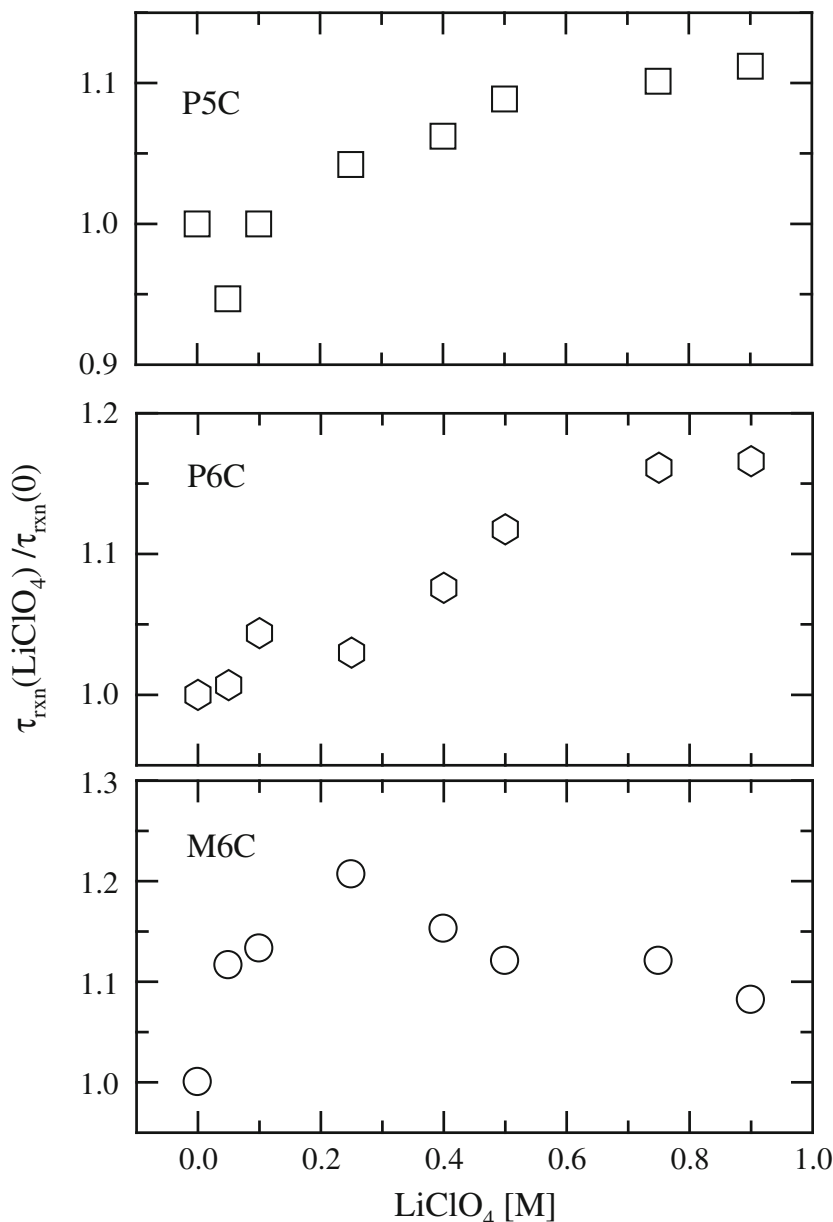


Figure 12. Electrolyte concentration dependence of reaction time constant in acetonitrile reverse micelles at a fixed W_s . Ratio between reaction time in the presence and absence of LiClO_4 , $\tau_{rxn}(\text{LiClO}_4)/\tau_{rxn}(0)$, for the LE \rightarrow CT conversion reaction of P5C, P6C and M6C in AOT/n-heptane/acetonitrile reverse micelles at $W_s = 5$ are shown as a function of LiClO_4 concentration. The squares, hexagons and circles represent data respectively for P5C, P6C and M6C. Error associated with the reaction time constants is typically $\pm 5\%$ of the reported values.

pool size, $W_s = 5$. It is interesting to note that τ_{rxn} increases linearly with LiClO_4 concentration for P5C and P6C but exhibits a non-monotonic dependence for M6C. Note a pronounced non-monotonic LiClO_4 concentration dependence of τ_{rxn} was also observed earlier in bulk ethyl acetate with another closely related molecule of the PnC series.⁴⁵ Data in figure 12 indicate τ_{rxn} increases only by $\sim 15\%$ for P5C and $\sim 20\%$ for P6C at highest LiClO_4 concentration over their respective values in the absence of any electrolyte at $W_s = 5$. The peak value of τ_{rxn} for M6C is again $\sim 20\%$ larger than that in the absence of LiClO_4 . This is surprising given the fact that the viscosity increases by nearly a factor of 2 in this concentration range (see figure 3). A much less lengthening of τ_{rxn} than expected on viscosity consideration probably suggests electrolyte-induced enhancement of solution polarity⁴² facilitating the ICT reaction in confined electrolyte solutions, leading to a partial decoupling from the local viscosity. This possibility, however, does not explain why the dependence of τ_{rxn} on electrolyte concentration shows a maximum for M6C but linear for other two reactants. The plots of $\ln[\tau_{rxn}^{-1}]$ versus the reaction driving force ($-\Delta G_r$) do not indicate any different dependence for these three molecules and thus possibly rules out hidden role for reorganization energy (λ_s)⁴⁶ specific to any particular reactant among these three. The origin of different electrolyte concentration dependence of τ_{rxn} for M6C at this W_s of AOT/heptane/acetonitrile reverse micelles are unknown to us at present and thus further studies are required to better understand this phenomenon.

4. Conclusions

The summary of the present work is as follows. The pool size dependence of LE \rightarrow CT conversion reaction of photo-excited P5C, P6C and M6C in AOT/n-heptane/acetonitrile and AOT/n-heptane/methanol reverse micelles has been studied at room temperature. Absorption and fluorescence emission spectra of dissolved probe exhibit continuous red-shift with W_s , suggesting increase in polar solvent pool with it. Careful comparison of spectra taken at both smallest and largest W_s values, and those in binary saturated solutions of polar and non-polar solvents reveals no partitioning of polar solvent and solute into the non-polar phase of reverse micelles. In addition, formation of CT emission band shows gradual increase with W_s . Depending upon W_s , the formation of the more polar charge-transferred (CT) state in these confined environments has been found to be decreased by 10–100

times compared to that observed in bulk solvents. The rate constant for this conversion reaction has also been found to be slowed down by 1–2 orders of magnitude. In order to correlate the observed equilibrium and time-dependent aspects of the ICT reaction with solvent properties, dielectric constant, viscosity and average solvation time have been estimated by following the fluorescence response of a non-reactive probe dissolved in these confined media. At $W_s = 5$ for both acetonitrile and methanol, the estimated dielectric constants are found to be 3–5 times less than the bulk values. Slope of increase of dielectric constant with W_s is steeper for confined methanol than that for confined acetonitrile but similar to that for confined water. The ‘local’ viscosity also increases by a factor of 2 at this W_s for acetonitrile. Measured average solvation times are found to be at least three orders of magnitudes slower than those measured for bulk solvents. The reduction in rate constant by 1–2 orders of magnitude is argued to originate from the decreased solution polarity, enhanced local viscosity and slow solvent reorganization in these confined solvents.

Subsequently, electrolyte effects on an ICT reaction in confined environment, has been investigated at a fixed W_s for acetonitrile reverse micelles. A maximum of $\sim 20\%$ lengthening of the reaction time constant over the value in the absence of electrolyte (LiClO_4) has been observed in the concentration range of 0.0–0.9 M. While the reaction time constant for P5C and P6C increases linearly with electrolyte concentration in confined polar solvent, it shows a non-monotonic LiClO_4 concentration dependence for M6C. Similar non-monotonic dependence is also observed for measured average solvation time but the estimated viscosity varies between 2 and 4 times of the bulk value. Much less reduction in reaction rate constant than expected from the viscosity consideration suggests more complex medium effects on ICT reaction in confined electrolyte solutions. The correlation between the reaction rate and reaction driving force has been found to be, on an average, linear for all these ICT molecules in both the presence and absence of electrolyte in this concentration range. We are, therefore, yet to understand the origin of non-monotonic electrolyte concentration dependence of ICT reaction rate constant in M6C.

The role of solute-medium interaction and medium dynamics can be further explored by following the reaction in binary liquid mixtures, molten non-aqueous electrolyte mixtures and solution pH dependence. In non-aqueous multi-component electrolyte mixtures⁹⁶ one would like to investigate the common ion effects on equilibrium constant and time scale of an ICT

reaction. Presence of proton in solution may influence the availability of the electron pair in the donor moiety for participation in the charge transfer process. Preferential solvation and diffusive time scale of solvent rearrangement in the first few solvation shells around a reactant may lead to more complex effects on ICT reaction than in neat solvents. Temperature dependent studies of ICT reaction in media, where heterogeneity rules the solution structure (for example, aqueous mixtures of tertiary butanol) may also provide important information about the role of solution structure on ICT reaction.

Acknowledgements

We thank Ms. S Sengupta and Dr. N Rohman for their help at the initial stage of this work. Financial support from the Council of Scientific and Industrial Resource (CSIR), India is gratefully acknowledged.

Supporting information

Tables S1–S3 and figures S1–S4 were provided as supplementary materials. See www.ias.ac.in/chemsci for supporting information.

References

- Luisi P L and Straub B E (eds) 1984 *Reverse micelles: Biological and technological relevance to amphiphilic structures in apolar media* (Plenum: New York)
- Levinger N E 2002 *Science* **298** 1722
- Willard D M, Riter R E and Levinger N E 1998 *J. Am. Chem. Soc.* **120** 4151; (b) Riter R E, Undiks E P and Levinger N E 1998 *J. Am. Chem. Soc.* **120** 6062; (c) Riter R E, Willard D M and Levinger N E 1998 *J. Phys. Chem. B* **102** 2705
- Harpham M R, Ladanyi B and Levinger N E 2005 *J. Phys. Chem. B* **109** 16891
- Menger F M, Donohue J A and Williams R F 1973 *J. Am. Chem. Soc.* **95** 286; (b) Menger F M and Yamada K 1979 *J. Am. Chem. Soc.* **101** 6731
- Bhattacharyya K 2003 *Acc. Chem. Res.* **36** 95; (b) Bhattacharyya K and Bagchi B 2000 *J. Phys. Chem. A* **104** 10603; (c) Ghosh S, Mandal U, Adhikari A, Dey S and Bhattacharyya K 2007 *Int. Rev. Phys. Chem.* **26** 421
- Baruah B, Roden J M, Sedgwick M, Correa N M, Crans D C and Levinger N E 2006 *J. Am. Chem. Soc.* **128** 12758
- De T and Maitra A 1995 *Adv. Colloid Interface Sci.* **59** 95
- Silber J J, Biasutti A, Abuin E and Lissi E 1999 *Adv. Colloid Interface Sci.* **82** 189
- Biswas R, Rohman N, Pradhan T and Buchner R 2008 *J. Phys. Chem. B* **112** 9379
- Rico I and Lattes A 1984 *J. Colloid Interface Sci.* **102** 285
- Ray S and Moulik S P 1994 *Langmuir* **10**, 2511
- Hayes D G and Gulari E 1995 *Langmuir* **11** 4695
- Gautier M, Rico I, Samii A-Z, De Savignac A and Lattes A J 1986 *J. Colloid Interface Sci.* **112** 484
- Mukherjee K, Moulik S P and Mukherjee D C 1993 *Langmuir* **9** 1727
- Mukherjee K, Mukherjee D C and Moulik S P 1994 *J. Phys. Chem.* **98** 4713
- Correa N M and Levinger N E 2006 *J. Phys. Chem. B* **110** 13050
- Shirota H and Segawa H 2004 *Langmuir* **20** 329
- Riter R E, Kimmel J R, Undiks E P and Levinger N E 1997 *J. Phys. Chem. B* **101** 8292
- Falcone R D, Correa N M, Biasutti M A and Silber J J 2000 *Langmuir* **16** 3070
- Falcone R D, Silber J J and Correa N M 2009 *Phys. Chem. Chem. Phys.* **11** 11096
- Novaira M, Moyano F, Biasutti M A, Silber J J and Correa N M 2008 *Langmuir* **24** 4637; (b) El Seoud O A, Correa N M and Novaki L P 2001 *Langmuir* **17** 1847; (c) Novaki L P, Correa N M, Silber J J and El Seoud O A 2000 *Langmuir* **16** 5573
- Mathew C, Saidi Z, Peyrelasse J and Boned C 1991 *Phys. Rev. A* **43** 873
- Lopez-Cornejo P and Costa S M B 1998 *Langmuir* **14** 2042
- Laia C A T, Lopez-Cornejo P, Costa S M B, d'Oliveira J and Martinho J M G 1998 *Langmuir* **14** 3531
- Friberg S E, Rong G and Ward A J I 1988 *J. Phys. Chem.* **92** 7247
- Shchipunov Y A and Shumilina E V 1996 *Colloid J.* **58** 123
- Rico I and Lattes A 1987 In *Microemulsion systems* Rosano H L and Clausse M (eds) (New York: Marcel Dekker) Vol. 24
- Mukherjee L, Mitra N, Bhattacharya P K and Moulik S P 1995 *Langmuir* **11** 2866
- Chhabra V, Lal M and Maitra A N 1995 *J. Mater. Res.* **10** 2689
- Singhal M, Chhabra V, Kang P and Shah D O 1997 *Mater. Res. Bull.* **32** 239
- Venables D S, Huang K and Schmuttenmaer C A 2001 *J. Phys. Chem. B* **105** 9132
- Setua P, Seth D and Sarkar N 2009 *Phys. Chem. Chem. Phys.* **11** 8913
- Shirota H and Horie K 1999 *J. Phys. Chem. B* **103** 1437
- Hazra P, Chakrabarty D and Sarkar N 2002 *Chem. Phys. Lett.* **358** 523
- Hazra P and Sarkar N 2002 *Phys. Chem. Chem. Phys.* **4** 1040
- Hazra P, Chakrabarty D and Sarkar N 2002 *Langmuir* **18** 7872
- Hazra P, Chakrabarty D and Sarkar N 2003 *Chem. Phys. Lett.* **371** 553
- Binks B P, Kellay H and Meunier J 1991 *Europhys. Lett.* **16** 53
- Yagmur A, Asrein A, Antalek B and Gartri N 2003 *Langmuir* **19** 1063
- Tsao H K 1999 *Langmuir* **15** 4981
- Huppert D, Ittah V and Kosower E M 1989 *Chem. Phys. Lett.* **159** 267

43. Novaira M, Biasutti M A, Silber J J and Correa N M 2007 *J. Phys. Chem. B* **111** 748
44. Pradhan T, Biswas R 2007 *J. Phys. Chem. A* **111** 11524
45. Pradhan T and Biswas R 2009 *J. Solution Chem.* **38** 517
46. Pradhan T, Gazi H A R and Biswas R 2009 *J. Chem. Phys.* **131** 054507
47. Riddick J A, Bunger W B and Sakano T K 1986 *Organic solvents* (New York: Wiley)
48. Dahl K, Biswas R, Ito N and Maroncelli M 2005 *J. Phys. Chem. B* **109** 1563
49. Pradhan T, Gazi H A R and Biswas R 2010 *J. Chem. Sci.* **122** 481; (b) Gazi H A R and Biswas R 2011 *J. Chem. Sci.* **123** 265
50. Grabowski Z R, Rotkiewicz K and Rettig W 2003 *Chem. Rev.* **103** 3899
51. Lippert E, Rettig W, Bonacic-Koutecky V, Heisel F and Mieche J A 1987 *Adv. Chem. Phys.* **68** 1
52. Hicks J, Vandersall M, Babarogic Z and Eisenthal K B 1985 *Chem. Phys. Lett.* **116** 18
53. Hicks J, Vandersall M T, Sitzmann E V and Eisenthal K B 1987 *Chem. Phys. Lett.* **135** 413
54. Nag A, Kundu T and Bhattacharyya K 1989 *Chem. Phys. Lett.* **160** 257
55. Horng M L, Gardecki J A, Papazyan A and Maroncelli M 1995 *J. Phys. Chem.* **99** 17311
56. Biswas R, Lewis J E and Maroncelli M 1999 *Chem. Phys. Lett.* **310** 485
57. Reynolds R, Gardecki J A, Frankland S J V, Horng M L and Maroncelli M 1996 *J. Phys. Chem.* **100** 10337
58. Hynes J T 1994 *Charge-transfer reactions and solvation dynamics in ultrafast dynamics of chemical systems* Simon J D (ed) (Dordrecht: Kluwer) p. 345
59. van der Zwan G and Hynes J T 1991 *Chem. Phys.* **152** 169
60. Krishna M M G 1999 *J. Phys. Chem. A* **103** 3589
61. Rettig W J 1980 *J. Lumin.* **26** 21
62. Rettig W 1982 *J. Phys. Chem.* **86** 1970
63. Zachariasse K A, Grobys M, von der Haar T, Hebecker A, Il'ichev Y V, Jiang Y-B, Morawski O and Kuhnle W 1996 *J. Photochem. Photobiol. A* **102** 59
64. Zachariasse K A 2000 *Chem. Phys. Lett.* **320** 8
65. Zachariasse K A, Druzhinin S I, Bosch W and Machinek R 2004 *J. Am. Chem. Soc.* **126** 1705
66. Techert S and Zachariasse K A 2004 *J. Am. Chem. Soc.* **126** 5593
67. Pradhan T and Biswas R 2007 *J. Phys. Chem. A* **111** 11514
68. Pradhan T, Ghoshal P and Biswas R 2008 *J. Phys. Chem. A* **112** 915
69. Pradhan T, Ghoshal P and Biswas R 2009 *J. Chem. Sci.* **121** 95
70. Lewis J E, Biswas R, Robinson A G and Maroncelli M 2001 *J. Phys. Chem. B* **105** 3306
71. Lakowicz J R 1999 *Principles of fluorescence spectroscopy*, 2nd edn (New York: Kluwer Academic/Plenum Publishers)
72. Maroncelli M and Fleming G R 1987 *J. Chem. Phys.* **86** 6221
73. Chapman C F and Maroncelli M 1991 *J. Phys. Chem.* **95** 9095
74. Horng M L, Gardecki J A and Maroncelli M 1997 *J. Phys. Chem. A* **101** 1030
75. Zhu D-M, Wu X and Schelly Z A 1992 *J. Phys. Chem.* **96** 7121
76. Senapati S and Chandra A 2001 *J. Phys. Chem. B* **105** 5106
77. Senapati S and Chandra A 1999 *J. Phys. Chem. B* **111** 1223
78. Gray C G and Gubbins K E 1984 *Theory of molecular fluids* (Oxford: Clarendon) Vol. I
79. Hansen J P and McDonald I R 1976 *Theory of simple liquids* (Academic Press)
80. Ghosh S, Ramanathan K V and Sood A K 2004 *Europhys. Lett.* **65** 678
81. Koga K, Gao G T, Tanaka H and Zeng X C 2001 *Nature* **412** 802; (b) Koga K, Gao G T, Tanaka H and Zeng X C 2002 *Physica* **314** 462
82. Marti J and Gordillo M C 2001 *Phys. Rev. E* **64** 021504; (b) Gordillo M C and Marti J 2000 *Chem. Phys. Lett.* **329** 341
83. Sansom M S P and Biggin P C 2001 *Nature* **414** 156
84. Hummer G, Rasiah J C and Noworyta J P 2001 *Nature* **414** 188
85. Sando G M, Dahl K and Owrutsky J C 2005 *J. Phys. Chem. B* **109** 4084
86. Biswas R, Das A R, Pradhan T, Touraud D, Kunz W and Mahiuddin S 2008 *J. Phys. Chem. B* **112** 6620
87. Bagchi B and Biswas R 1999 *Adv. Chem. Phys.* **109** 207
88. Fee R S and Maroncelli M 1994 *Chem. Phys.* **183** 235
89. Note that the above correlation, which has been constructed from the room temperature liquid data, may not quantitatively represent the viscosity dependence of solute rotation in spatially heterogeneous media such as those inside reverse micelles. In the absence of any simple yet better description, the same correlation has been used to estimate local viscosity experienced by a probe trapped in polar solvent pool.
90. Biswas R and Bagchi B 1997 *J. Chem. Phys.* **106** 5587
91. Hartman R S, Konitsky W M and Waldeck D H 1993 *J. Am. Chem. Soc.* **115** 9692
92. Kumar P V and Maroncelli M 2000 *J. Chem. Phys.* **112** 5370
93. Kurnikova M G, Balabai N, Waldeck D H and Coalson R D 1998 *J. Am. Chem. Soc.* **120** 6121
94. Kurnikova M G and Waldeck D H 1996 *J. Chem. Phys.* **105** 628
95. Changes in 'local viscosity' borne out by the rotation data summarized in references 34 and 35 become more quantitative if the initial anisotropy $r(0)$ values are fixed.
96. Guchhait B, Gazi H A R, Kashyap H K and Biswas R 2010 *J. Phys. Chem. B* **114** 5066; (b) Gazi H A R, Guchhait B, Daschakraborty S and Biswas R 2011 *Chem. Phys. Lett.* **501** 358